ON QUANTUM PHENOMENA IN MODERN PHYSICS

A. BAKSHI
Data Analyst, Experiment Designer

M. CHEN
Experiment Designer

J.HUANG
Data Analyst

J. LIN
Data Analyst

J. LIU
Experiment Designer

(Received on January 17, 2018)

Modern physics, the study of natural phenomena which resists classical explanations, has received considerable attention of late in both scientific and amateur media. This report compiles various effects relating properties of light known since antiquity and quantum ideas theorized in the late twentieth century, includingcomputation of Plancks constant to be (6.5.9)Js and derivation of the uncertainty principle: $\sigma_y \cdot \sigma_{P_y} = h$. The efficiency of the tested LEDs was also analyzed, and due to the inefficiencies in semiconductors, (3.8.7) E-20 J of energy was lost as heat per electron. Theoretical models have been applied to camera technology, including suggestions to improve camera sensor accuracy and calibration.

I INTRODUCTION

The structure of light is one of the few remaining questions posed since antiquity and humanity has still been unable to answer. This report is not intended to solve this mystery, but rather to submit evidence to the collective theories mankind is developing.

II THEORY

As the experiments performed dealt with light, several equations were needed for reliable analysis. These equations describe the relationships between frequency, energy, and wavelength of a desired light source.

$$E = hf \qquad [1]$$

(*HRW 2017*)

Where:

E = the energy of photon (J)
h = Planck's Constant
f = the frequency of the radiation (Hz)

$$c = \lambda f \qquad [2]$$

(*HRW 2017*)

Where:

c = the speed of light (ms^{-1})
λ = the wavelength (m)

Analysis of a semi-conductor was also performed. As there is a gap across the valence and conduction bands, a certain energy threshold must be met for an electron to cross over. This is modeled by:

$$E_{BG} = eV_T \qquad [3]$$

(*HRW 2017*)

Where:

E_{BG} = the energy required (J)
e = elementary charge (C)
V_T = the threshold potential (V)

The de Broglie equation was also used, as it relates the wavelength of a moving particle to its momentum, as described below.

$$h = p\lambda \qquad [4]$$

(*HRW 2017*)

Where:

p = the momentum of the particle (kgms^{-1})

Finally, two equations were used to describe the black body curve of the lightbox: Planck's Equation, and Wien's Law.

$$I(\lambda, T) = \frac{2hc^2}{\lambda^5} \frac{1}{e^{\frac{hc}{\lambda kT}} - 1}. \quad [5]$$

(*HRW 2017*)

Where:
I = the radiance ($Wm^{-1}sr^{-1}$)
T = the temperature (K)
k = Boltzmann constant

$$\lambda_{max} T = b \quad [6]$$

(*HRW 2017*)

Where:
λ_{max} = the peak wavelength (nm)
b = Wien's constant

III Method

A Canon 6D with a known spectral response was used to find the wavelength of the LEDs.

Colour	Wavelength(nm)
UV	422±3
Blue	472±1
Green	520±4
Yellow	593±1
Orange	601±3
Red	667±2

Fig. 1. Table of Measured LED Wavelengths Taken with Canon 6D and measured through hue.

The electrons within the semiconductor can be energized by applying an external electromotive force. Three methods were employed to find the threshold potential V_T.

The LEDs' threshold potential was found by first by observing it and then by analyzing its V-i curve. The most precise measurement for threshold potential was obtained by discharging a capacitor across an LED. The LED's resistance quickly increases when the potential approaches its threshold due to its V-i characteristics, which consequently increases the time constant. This large resistance effectively stagnates the discharge of the capacitor. The potential across the capacitor was measured and graphed, and the stagnation potential was taken to be the LEDs threshold potential.

For the single slit experiment, a helium neon laser was used to regulate parallel light rays with constant wavelengths. The imaging technology used in the rest of the lab was kept consistent. The raw images were processed with GIMP and Lightroom, and analyzed with the aid of scripts written in both Java and MatLab.

For the final experiment, a lightbox was set up with a grading filter. An HDR image was generated using a Canon 6D chip manual found online. However, since the legality and reliability of the colour response wasn't deemed up to par, several more response tests were conducted to ensure the colour calibration was correct. This included the 4-Colour Test, as well as extensive use of a Colour Passport, under sunlit conditions. These values were then compared to Lightroom presets, and adjusted accordingly.

IV Analysis

An LED works on the same principles as all other diodes. Within the LED, a chip created with doped semiconductor material acts as a p-n junction. While forward biased, electrons flow from the n-doped region to the p-doped region, filling in the so-called holes. When this occurs in the semiconductors found in LEDs, a phenomenon known as electroluminescence occurs, whereby the semiconductor emits light.

In a p-n doped semiconductor, free electrons are in the conduction band while the

holes are in the valence band. The gap between these bands is called the band gap. For an electron to cross this gap, it must have an energy above a certain threshold. Using the relationship [1], the constant relating E and f, known as Planck's constant, can be found.

Using the measured wavelength and [2], the frequency of the LEDs was determined. The plot of E_{BG} vs. f using data from the capacitor configuration is shown below.

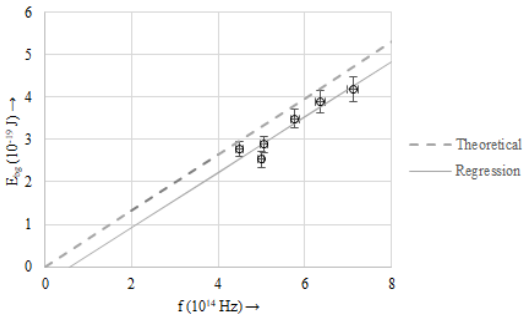

Fig. 2. The energy required to cross the band gap vs the frequency of light emitted. The regressed and theoretical lines were also plotted. This graph has a slope similar to the theoretical slope, but has a vertical shift due to energy lost as heat. This data was collected using the capacitor method.

The equation regressed via LINEST was:

$$E_{BG} = (6.5 \pm .9)\text{E}{-}34 \cdot f - (3.8 \pm .7)\text{E}{-}20 \quad [7]$$

The Planck's constant h using all three methods are summarized below.

Method	Planck's Constant (E-34 Js)
Visual	8±2
Variable Resistor V-i curve	7±1
Discharging Capacitor	6.5±.9

Fig. 3. Table displaying the Planck's constant calculated with different methods.

Since the band gap is an intrinsic feature of the material, the amount of energy needed to cross this gap does not change as more potential is applied. However, if there is a larger potential difference across the semiconductor, the emitted photons may have energies that are different from the energy needed to cross the band gap, which results in the creation of heat. This heat is absorbed by lattice vibrations in the semiconductor known as phonons.

This heat is evident in Fig 2 by the vertical shift in the regressed equation. The shift is the result of the heat dissipated in the semiconductor. As most LEDs have a similar heat generation near their threshold potentials, the vertical shift of $(3.8 \pm .7)\text{E}{-}20$ J is a good approximation of the heat loss per electron crossing the band gap of this particular manufacturers LEDs.

Theoretically, it is possible for an LED to remove heat from the semiconductor lattice which would make the LED more than 100% efficient. (Santhanam, 2012). Graphically, this would result in a constant that is greater than 0.

The diffraction of light through a very thin slit can be explained by classical mechanics, specifically by examining the wave properties of light. The same analysis yielded an (albeit weaker) derivation of the Heisenberg Uncertainty Principle.

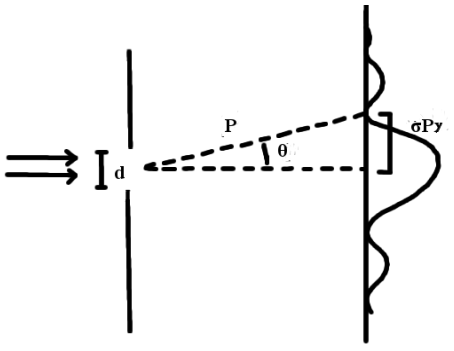

Fig. 4. Cross section of single slit diffraction. Parallel rays of light enter from the left of the figure, and contrary to classical intuition, diffuses, and creates a pattern along the right side.

The location of the first dark fringe is well known, and given by [8].

$$\sigma_{P_y} = p \cdot \sin\theta \quad [8]$$

Where:
θ = angle of first dark fringe
σ_{P_y} = standard deviation of momentum in y

Specific information is known about a photon as it passes through the single slit, namely, its position. This becomes a crude representation of Heisenberg's uncertainty principle, which follows.

$$\sigma_y \cdot \sigma_{P_y} = \frac{h}{4\pi} \qquad [9]$$

Where:
σ_y = standard deviation of photon position

Some further algebra was employed to verify the theory, as σ_{P_y} is rather difficult to measure directly. The end result substituted back into [4] gave

$$\frac{d}{\lambda} \sin\left(\arctan\left(\frac{A}{2D}\right)\right) = 1 \qquad [10]$$

Where:
D = distance between the slit and the wall (m)
A = distance between two dark fringes (m)

Experimentally obtained values λ=(630 $\pm$ 30) nm and D=(364 $\pm$ .2)mm was then substituted, and with the addition of manufacturer provided values for the slit width, the LHS of [10] was computed.

Index	d(μm)	A(mm)	LHS of [10]
1	88	5.2±.2	1.03±.05
2	176	2.6±.2	1.07±.05

Fig. 5. Verifying the derived uncertainty principle The LHS of [10] was computed to be very close to 1 in both scenarios, which is further evidence of the uncertainty principle.

The intensity profiles of a Canon 6D were also created, allowing the colour response to be more accurate than otherwise.

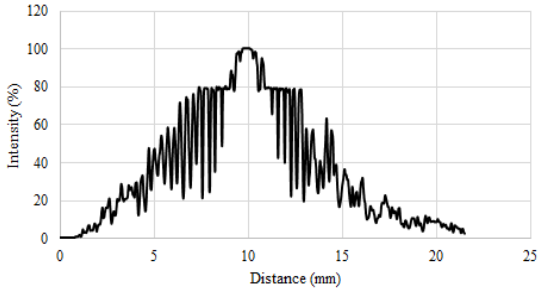

Fig. 6. Intensity (as a percentage of max) vs position. The intensity was calculated as a weighted average of the RGB values based off of the wavelength of the laser, which corresponded to an ideal hex code of #FF4200.

Further, the locations of the dark fringes were compared to their theoretical counterparts, and were within a margin of error.

Index	Theoretical Position (mm)	Measured Position (mm)
1	-5.2±.1	-5.2±.2
2	-2.61±.05	-2.6±.2
3	2.61±.05	2.7±.2
4	5.2±.1	5.2±.2

Fig. 7. Theoretical vs Measured Positions of Dark Fringes. Theoretical values were computed with a generalized Fig. 3 and experimental values were numerically obtained with a computer script.

It is welcoming to note that the 6D has an extremely accurate colour sensor, even without calibration. This is especially when the uncalibrated hue of the blue LED matched very closely to the theoretical value.

Even so, the edited version of the picture also had to be tested. As such, the following pixel analysis was conducted.

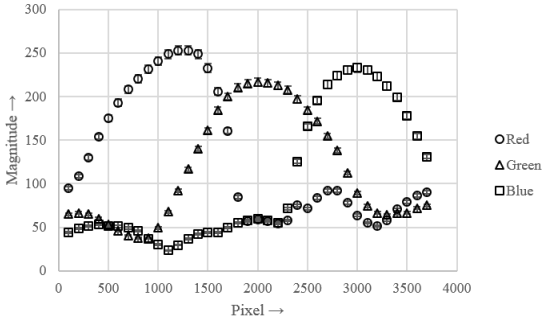

Fig. 8. RGB Values of pixels. RGB peaks remain relatively equal after corrections.

While it should be expected that the tail ends of the curves should approach 0, this was not the case. This was concluded to be the undertones of the paper underneath.

It is interesting to note that there were generally high green undertones that needed to be fixed, more than other colours. According to Wang et al (2016), this is due to the fact that, in an attempt to lower the possible effects of chromatic aberration of bad lenses, cameras often undercompensate on reds and blues, and overcompensate on greens. Of course, this gently affects the colouration when not affected, but it is a trade companies are willing to make.

The radiance was found as a function of the deflection angle, and was plotted against both colour and deflection angle.

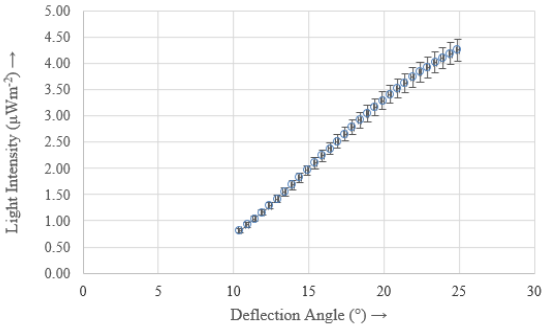

Fig. 9. Intensity v. Deflection Angle. Note the general increase. However, no peak is evident.

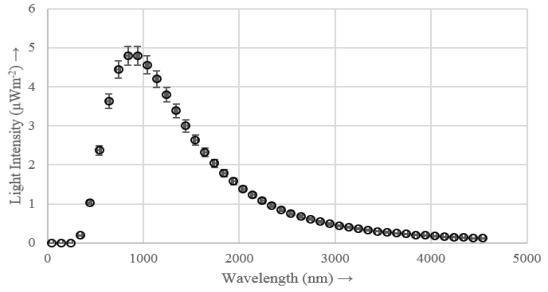

Fig. 10. Intensity v. Wavelength. A more complete image of Fig. 9. A peak is visible at 885nm.

Using a FLIR infrared camera, extra measurements were taken, and values were matched with those from [5]. This gave a much more complete picture of the curve than in Fig. 9. In Fig. 10, the black body curve is evident, as is the peak, at a wavelength beyond the spectrum of visible light.

Using [6], it can then be determined that the temperature of the bulb is (3273 ± 20)K.

The 6D itself was used to calculate the colour temperature of the bulb. Using the white balance and histogram settings, the overall composition had balance at 3300K.

A suggestion could be derived from this experiment. Knowing that the white balance sensor is generally efficient at taking measurements, it can be used to measure a light mounted in the camera. The sensors can image a spectrum directly built into the camera and compared with theoretical results of the white balance sensor.

V Sources of Error

The uncertainty principle affirms an inevitability in the universe: an observer cannot be certain of anything. This report, without flawless equipment or methodology, does much worse.

Further, certain logical errors exist. The uncertainty principle has been derived from the single slit experiment, but in no way has it been proven. There exist many explanations for the diffraction effect, and this report serves only as evidence for modern theories.

VI Conclusion

The results of this report have many practical applications, including implementations in display technology, and cameras, as well as in other disciplines of science such as chemistry. Next steps include stronger evidence for the uncertainty principle, as well as deeper experimental imaging tests.

VII Sources

van Bemmel, H. "AP Lab Manual" 2017

Halliday, D., Resnick, R., & Walker, "Fundamental of Physics." 2001.

Santhanam, P., Gray, D. J., & Ram, R. J, "Thermoelectrically Pumped Light-Emitting Diodes Operating above Unity Efficiency." 2012.

Wang, P., Mohammad, N., & Menon, "Chromatic aberration corrected diffractive lenses" 2016.